

Memory in Self Organized Criticality

Eugenio Lippiello,¹ Lucilla de Arcangelis² and Cataldo Godano³¹ INFN, Udr Naples and University of Naples "Federico II", 80125 Napoli, Italy² Department of Information Engineering and INFN - Coherencia, Second University of Naples, 81031 Aversa (CE), Italy³ Department of Environmental Sciences and INFN, Second University of Naples, 81100 Caserta, Italy

Many natural phenomena exhibit power law behaviour in the distribution of event size. This scaling is successfully reproduced by Self Organized Criticality (SOC). On the other hand, temporal occurrence in SOC models has a Poisson-like statistics, i.e. exponential behaviour in the inter-event time distribution, in contrast with experimental observations. We present a SOC model with memory: events are nucleated not only as a consequence of the instantaneous value of the local field with respect to the firing threshold, but on the basis of the whole history of the system. The model is able to reproduce the complex behaviour of inter-event time distribution, in excellent agreement with experimental seismic data.

After the pioneering work of Bak, Tang and Wiesenfeld [1], Self Organized Criticality (SOC) has been proposed as a successful approach to the understanding of scaling behaviour in many natural phenomena. The term SOC usually refers to a mechanism of slow energy accumulation and fast energy redistribution driving the system toward a critical state. The prototype of SOC systems is the sand-pile model in which particles are randomly added on a two dimensional lattice. When the number of particles n_i in the i -th site exceeds a threshold value n_c , this site is considered unstable and particles are redistributed to nearest neighbor sites. If in any of these sites $n_j > n_c$, a further redistribution takes place propagating the avalanche. Border sites are dissipative and discharge particles outside. The system evolves toward a critical state where the distribution of avalanche sizes is a power law obtained without fine tuning: no tunable parameter is present in the model. The simplicity of the mechanism at the basis of SOC has suggested that many physical and biological phenomena characterized by power laws in the size distribution, represent natural realizations of the SOC idea. For instance, SOC has been proposed to model earthquakes [2,3], the evolution of biological systems [4], solar flare occurrence [5], fluctuations in confined plasma [6] snow avalanches [7] and rain fall [8].

Moreover, SOC models can be also considered as cellular automata generating stochastic sequences of events. An important quantity showing evidence of time correlations in a sequence is the distribution of time intervals between successive events. Denoting t as the time elapsed between the end of an avalanche and the starting of the next one, for the sand-pile model one obtains that t is exponentially distributed [9]. This behaviour reveals the absence of correlations between events typical of a Poissonian process. Conversely the inter-event time distribution $N(t)$ of many physical phenomena has a non-exponential shape, as for instance in the case of earthquakes [10], solar flares [9] and confined plasma [11]. The failure in the description of temporal occurrence is generally considered the main restriction for the applicability of SOC ideas to the description of the above phenomena.

In this letter we address the problem of introducing time correlations within SOC and, in order to validate our model, we compare our results with experimental records from seismic catalogs. Seismicity is considered here as a typical physical process with power law in the size distribution but also strong correlations between events. In this case, the sand pile model can be directly mapped [12-14] in the Burridge-Knoppe model, proposed for the description of earthquake occurrence. In this model a continental plate is represented as a series of blocks interconnected with each other and with a rigid driver plate by springs, then the quantity n_i represents the global force acting on the i -th block and n_c the threshold for slippage. We introduce memory within the SOC context: the local instability depends not only on the instantaneous value n_i but on the whole history of energy accumulation. Our memory ingredient is analogous to recent ideas [15] introduced for the understanding of earthquake interactions.

The first observation of correlations between earthquakes, dates back to Omori [16] who suggested that earthquakes tend to occur in clusters temporally located after main events: the number of aftershocks following a main event after a time t , $r(t)$, decays as a power law $r(t) \propto t^{-1}$. Furthermore, a large earthquake produces also an abrupt modification in seismic activity across a widespread area [17]. A striking example of this remote triggering mechanism is the Landers earthquake of magnitude 7.3 occurred in 1992, which triggered three hours later the 6.5 magnitude event in the town of Big Bear on a different fault, together with a general increase in activity across much of the Western United States. A clear understanding of the physical processes responsible for this behaviour is still lacking: the non-local triggering mechanism cannot be explained in terms of static stress changes responsible for aftershocks and one must invoke non linear interactions to modify the friction law on remote faults [17,19,18,15].

The inter-time distribution combines both the effect of the local clustering of the aftershocks sequence described by the Omori law, with the remote triggering mechanism involving larger distances. The presence of both features

give rise to an intertime distribution $N(t)$ that is not a power law but has a more complex shape [20]. Nevertheless, Corral has shown that this shape is quite independent on the geographical region and the magnitude range considered [10]. This observation indicates that $N(t)$ is a fundamental quantity to characterize the temporal distributions of earthquakes.

Here we introduce within SOC a non local mechanism for event nucleation. In our approach seismic fracture depends on a collective behaviour of the earth crust: the triggering of a new event is determined by the combined effect of the increase in the static stress together with the local weakening in a fault due to the loading global history. To this extent, we consider a square lattice of size L , each site being characterized not only by the value of the local stress σ_i but also by a site-counter c_i that represents the local memory. At $t = 0$ local stresses are assigned at random between $\sigma_c - z$ and σ_c , where z is the lattice coordination number and $\sigma_c > z$, whereas c_i is randomly set between zero and one. The simulation proceeds as follows. At each time t all sites are loaded with an uniformly increasing external stress, by adding one unit to all σ_i 's, and the local variable p_i is defined as

$$p_i = \frac{(\sigma_i - \sigma_c + z)}{z} \quad \text{if } \sigma_c - z < \sigma_i < \sigma_c \quad (1)$$

whereas $p_i = 1$ if $\sigma_i > \sigma_c$ and $p_i = 0$ if $\sigma_i < \sigma_c - z$. Then at each site the quantity $\sigma_i = \frac{(1 - c_i)}{p_i}$ is evaluated, measuring the local instability with respect to slippage, and its minimum value in the system, σ_{min} , is found. This value indicates the site most susceptible to seismic failure because of both the high local stress at that instant of time and the cumulated history of loads saved into the counters c_i . If σ_{min} is larger than a critical value σ_c , all counters are updated as

$$c_i^{new} = c_i^{old} + \sigma_{min} p_i \quad (2)$$

Then the external stress is uniformly loaded at constant rate and at each step the new value of σ_{min} in the system is evaluated and Eq.(2) applied. As soon as $\sigma_{min} < \sigma_c$, the site i with $\sigma_i = \sigma_{min}$ becomes the epicenter where the earthquake nucleates and its counter is set to zero. Other sites with $\sigma_{min} < \sigma_i < \sigma_c$ are considered stable unless involved in the fracture propagation. This choice is expression of fracture being a phenomenon controlled by the extreme value statistics.

When a site nucleates an earthquake, it discharges elastic energy uniformly by the transfer of a unit stress to all nearest neighbours, as in the sand pile model. The process goes on letting unstable sites, characterized by $\sigma_i < \sigma_c$, discharge energy and in this way propagating the seismic event farther and farther from the epicenter. The counters of all discharging sites are set to zero during the evolution, whereas counters of all other sites are updated at the end according to Eq.(2) with the actual value of σ_{min} . Energy back-flow allows to activate sites found stable during the forward propagation triggering further energy redistributions. At the end of the process the external load is increased again at constant rate until another event takes place.

The updating rule (2) is equivalent to consider a time dependent friction law [19], whose evolution is controlled not only by the local state at previous times but also by the instability condition for the whole system. Eq.(2) then introduces long range interactions and remote triggering by means of σ_{min} , since all sites in the system, even far from the epicenter, share this common information. The more a site is stressed (high p_i), the stronger it will react to this information. We have checked that our results are substantially unchanged if Eq.(2) is applied to a finite region of size $l < L$ centered in the site with $\sigma_i = \sigma_{min}$, for large enough l . A breaking rule similar to Eq. (2) has been successful in providing a good description of the propagation of stress corrosion cracks [21], a fracture process where local mechanical resistance of materials is weakened in time by chemical agents.

It is possible to calculate in a mean field approximation the fraction of active sites as function of time. This approximation is based on the assumption that the external stress is kept fixed and therefore can describe the behaviour of the system only at short time scales. As a consequence of this hypothesis, the fraction of active sites is related to the rate of occurrence of aftershocks, $r(t)$, happening over time scales shorter than the characteristic time of the loading mechanism. Let us consider at each time t and each site the quantity $q_i(t) = 1 - \sigma_i$ for $0 < \sigma_i < 1$ and $q_i(t) = 0$ for $\sigma_i > 1$. According to Eq.(2) one has, at constant load condition, that the value of $q_i(t)$ at the next time step is given by $q_i(t+1) = q_i(t) + \sigma_{min} p_i$, if the i -th site does not discharge energy and $q_i(t+1) = 0$ otherwise. Hence, the statistical average is

$$h q_i(t+1) = h q_i(t) + h \sigma_{min} p_i^s(t) \quad (3)$$

with $p_i^s(t)$ the probability for the site i to be stable at time t . Since, the spatial average, $q(t) = \frac{1}{L^2} \sum_{i=1}^{L^2} q_i(t)$, is an estimate of the fraction of sites that could become active at the next time step, $q(t)$ is the probability for a generic site to be unstable at time t and then $q(t) \approx 1 - p_i^s(t)$. In the hypothesis $\sigma_{min} \rightarrow \sigma_c$, valid for a system close to

trigger an event, one can neglect m_{in} in Eq.(3). Finally, supposing that $q_i(t)$ is a self-averaging quantity one has $q(t+1) \approx q(t) \approx q(t)$, which gives the Omori law $q(t) \propto t^{-1}$.

In order to evaluate the complete inter-time distribution $N(t)$, we numerically generate a large statistics of events and calculate the time distance between every couple of successive events involving more than one single site. Fig.1 shows, the experimental and the numerical data for $c = 0.9$ and $L = 500$. By re-scaling the numerical waiting time with an appropriate constant value, our data provide a very good agreement with the experimental distribution from the Southern California Catalogue [22], whereas the original SOC model exhibits exponential decay. We have monitored the behaviour of the distribution for different values of c (Fig.2): For $c = 0.3$, an exponential decay is observed whereas for intermediate values of c a complex behaviour starts to set in. For $c = 0.7$ the data follow a unique universal curve.

In order to fully validate the theoretical ideas of our model, we have also analyzed other statistical properties of seismic catalogues: energy and epicenters distance distributions. The energy release in an earthquake is expressed in terms of the magnitude, which is proportional to the logarithm of the fractured area A

$$M = k \log(A) + M_{in} \quad (4)$$

where M_{in} is a constant depending on the area units. The Gutenberg-Richter law implies that $N(M)$, the number of earthquakes with magnitude M , follows an exponential law [23]

$$N(M) \propto 10^{-bM} \quad (5)$$

where b is an experimental constant generally close to one. In order to compare our numerical results with experimental data, we evaluate the magnitude of an event using Eq. (4) with A being the number of discharging sites and $k \approx 0.65$ as for the Southern California Catalogue. The choice of the minimum magnitude M_{in} is arbitrary since it is related to the unit cell area, and in our case we set $M_{in} = 2$. The magnitude distribution, after an initial transient at small magnitudes ($M < 3$), follows the expected exponential behaviour of the Gutenberg-Richter law (Fig.3) over a magnitude range increasing with the system size L . Strong fluctuations observed at large M for small system sizes are finite size effects. The value of the best fit exponent b depends on the parameter c and becomes parameter independent for $c = 0.7$, where $b = 0.84$ (inset Fig.3). Comparing our numerical results with the data from the California Catalogue (Fig.4) good agreement is found between the experimental best fit value $b_{exp} = 0.86$ and numerical prediction. In the non conservative case, SOC also provides good agreement with the experimental size distribution [14].

Seismic catalogues also record the spatial coordinates of earthquake epicentres. We numerically evaluate the cumulative distribution of distance between all possible couple of events at a distance smaller than d , $N(d)$. We obtain a power law behaviour with an exponent equal to 1.84. Agreement with experimental data is observed for small distances. $N(d)$ calculated for the original SOC model provides similar results.

It is worth noticing that the behaviour of all experimental distributions is reproduced by numerical simulations without any fine tuning, i.e. numerical results are parameter independent for $c > 0.7$.

The complex seismic activity over large regions of the world is controlled by both local stress redistributions, generating aftershocks, and long range load transfer in the surrounding crust. In our approach these mechanisms are simply implemented in self-consistent local laws containing long range memory of stress history. A large event could then increase the seismic activity by inducing global weakening in the system, or else could even inhibit future earthquakes by resetting the local memory. This global memory ingredient could correspond to a variety of physical mechanisms inducing weakening in time for real faults [24], as stress corrosion [21], fault gauge deterioration [25] or pore pressure variation [26].

We have considered earthquake triggering as an example of physical problems in which time correlations are extremely important. We suggest that this SOC model with memory may be relevant for other physical phenomena described by a SOC approach and exhibiting a non-exponential decay in the inter-time distribution [9].

Acknowledgements. We would like to thank A. Coniglio, P. Gasparini and S. Nielsen for helpful discussions. This work is part of the project of the Regional Center of Competence "Analysis and Monitoring of Environmental Risk" supported by the European Community on Provision 3.16.

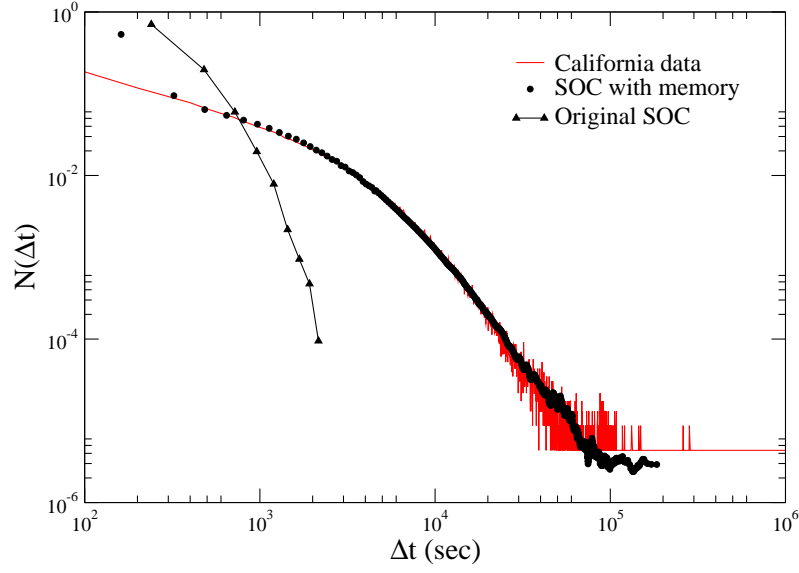


FIG .1. (Color online) The normalized waiting time distribution $N(\Delta t)$ between successive events for experimental and numerical data for our model and the original SOC model. Data for our model correspond to 2500 events in 3000 configurations of system size $L = 500$ with $\alpha_c = 0.9$. Time is measured in seconds and all numerical waiting times are rescaled by the constant factor 190.

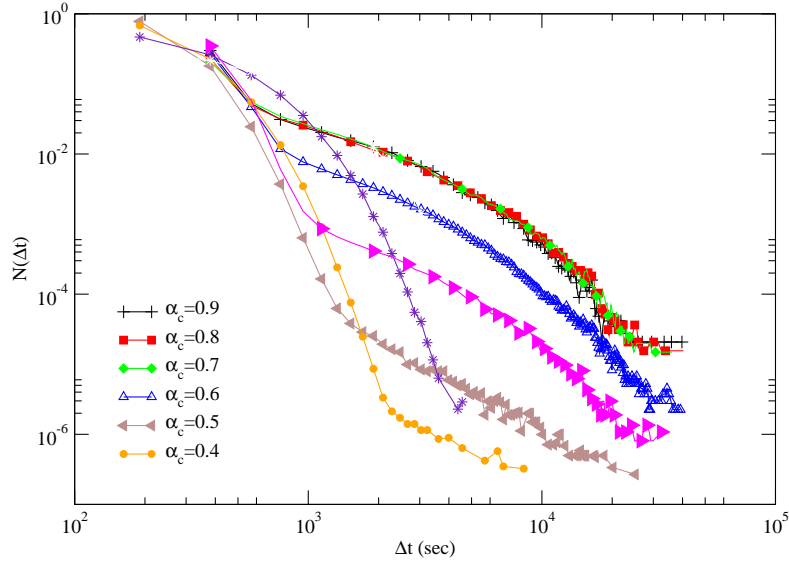


FIG .2. (Color online) Inter-event time distribution for 2500 events in 1000 configurations of system size $L = 100$ and different values of α_c .

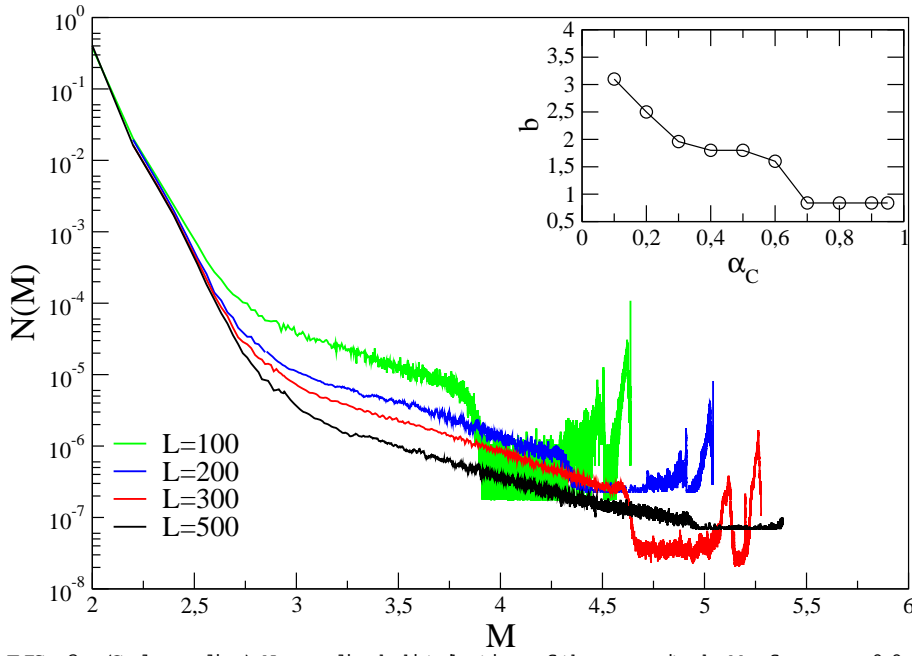


FIG. 3. (Color online) Normalized distribution of the magnitude M for $\alpha_c = 0.9$ and increasing lattice sizes L from top to bottom. The horizontal axis is due to single event statistics. In the inset we show the best fit exponent b of the

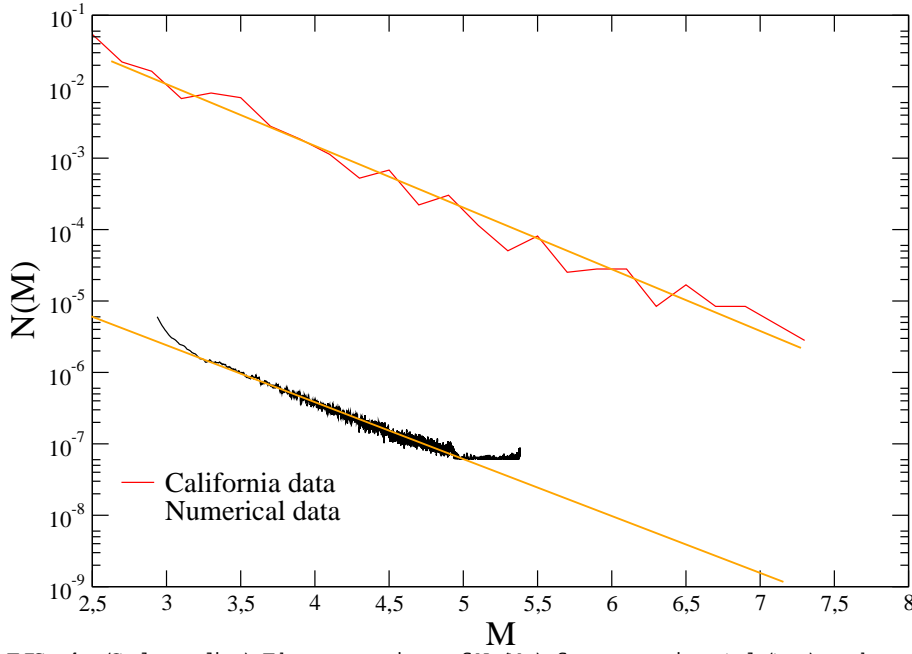


FIG. 4. (Color online) The comparison of $N(M)$ from experimental (top) and numerical data (bottom) for $L = 500$ and $\alpha_c = 0.9$. The average is taken over 3000 configurations of 2500 events each. Straight lines are the best fit curves $10^{-0.86M}$ and $10^{-0.84M}$ respectively.

[1] P. Bak, C. Tang, K. W. Wiesenfeld, Phys. Rev. Lett. 59, 381 (1987).

- [2] P.Bak, C.Tang, J. Geophys. Res. 94, 15635 (1989).
- [3] A.Somette, D.Somette, Europhys.Lett. 9, 197 (1989).
- [4] P.Bak, K.Sneppen, Phys. Rev. Lett. 71, 4083 (1993);
- [5] E.T.Lu, R.J.Hamilton, Astrophys. J. 380, L89 (1991); D.Hamilton, M.Nicodemi, H.J.Jensen A & A 387, 326 (2002);
D.Hughes et al Phys. Rev. Lett. 90, 131101 (2003);
- [6] P.A.Politzer, Phys. Rev. Lett. 84, 1192 (2000).
- [7] J.Faillettaz, F.Louchet, J.R.Grasso, Phys. Rev. Lett. 93, 208001 (2004).
- [8] O.Peters, C.Hertlein and K.Christensen, Phys. Rev. Lett. 88, 018701 (2002)
- [9] G.Botta, V.Carbone, P.Giuliani, P.Veltri, A.Vulpiani, Phys. Rev. Lett. 83, 4662 (1999);
- [10] A.Corral, Phys. Rev. Lett. 92, 108501 (2004).
- [11] V.Antoniet al, Phys. Rev. Lett. 87, 045001 (2001); E.Spada et al, Phys. Rev. Lett. 86, 3032 (2001).
- [12] K.Ito, M.Matsuzaki, J. Geophys. Res. 95, 6853 (1990).
- [13] S.R.Brown, C.H.Sholtz, J.B.Rundle, Geophys. Res. Lett. 18, 215 (1991); Nakanishi, H., Phys. Rev. A 43, 6613 (1991).
- [14] A.Olami, H.J.S.Feder, K.Christensen, Phys. Rev. Lett. 68, 1244 (1992)
- [15] R.S.Stein, Nature 402 605 (1999); T.Parson et al, Science 288, 661 (2000).
- [16] F.Omori, J. Coll. Sci. Imper. Univ. Tokio 7, 111 (1894); T.Utsu, Geophys. Mag. 30, 521 (1961).
- [17] D.P.Hill et al, Science 260, 1617 (1993).
- [18] In fact, these variations decrease with distance r from the source as r^{-3} and, for instance, in the case of the Landers earthquake the measured static stress change at a distance of 300 Km was less than 10^{-2} bar.
- [19] J.Deterich, J. Geophys. Res. 99, 2601 (1994).
- [20] M.S.Mega et al, Phys. Rev. Lett. 90, 188501 (2003), N.Scafetta, B.J.West Phys. Rev. Lett. 92, 138501 (2004).
- [21] H.J.Herrmann, J.Kertsz, L.de Arcangelis, Europhys.Lett. 10, 147 (1989).
- [22] Southern California Seismographic Network, <http://www.scec.org/ftp/catalogs/SCSN/>, including 366000 events with magnitude $M \leq 1$ from years 1975 to 2004.
- [23] B.Gutenberg, C.F.Richter, Bull. Seism. Soc. Am. 34, 185 (1944).
- [24] Y.Benn-Zion, J. Mech. Phys. Solids 49, 2209 (2001).
- [25] P.Mora, D.Place, S.Abe, S.Jouin, in Geocomplexity and the physics of earthquakes (AGU Publ. Washington, 2000) pp 105-126.
- [26] F.Mulargia, S.Castellaro, M.Ciccotti, Earthquake energy balance in Earthquake Science and Seismic Risk reduction (Kluwer Academic Publ. Dordrecht, 2003) p77.